High-frequency acoustic scattering from turbulent oceanic microstructure: The importance of density fluctuations

Andone C. Lavery,[a] Raymond W. Schmitt, and Timothy K. Stanton
Woods Hole Oceanographic Institution, Woods Hole, Massachusetts 02543

(Received 27 July 2002; accepted for publication 11 August 2003)

Acoustic scattering techniques provide a unique and powerful tool to remotely investigate the physical properties of the ocean interior over large spatial and temporal scales. With high-frequency acoustic scattering it is possible to probe physical processes that occur at the microstructure scale, spanning submillimeter to centimeter scale processes. An acoustic scattering model for turbulent oceanic microstructure is presented in which the current theory, which only accounts for fluctuations in the sound speed, has been extended to include fluctuations in the density as well. The inclusion of density fluctuations results in an expression for the scattering cross section per unit volume, σ_v, that is explicitly dependent on the scattering angle. By relating the variability in the density and sound speed to random fluctuations in oceanic temperature and salinity, σ_v has been expressed in terms of the temperature and salinity wave number spectra, and the temperature-salinity co-spectrum. A Batchelor spectrum for temperature and salinity, which depends on parameters such as the dissipation rates of turbulent kinetic energy and temperature variance, has been used to evaluate σ_v. Two models for the temperature-salinity co-spectrum have also been used. The predictions indicate that fluctuations in the density could be as important in determining backscattering as fluctuations in the sound speed. Using data obtained in the ocean with a high resolution vertical microstructure profiler, it is predicted that scattering from oceanic microstructure can be as strong as scattering from zooplankton. © *2003 Acoustical Society of America.*
[DOI: 10.1121/1.1614258]

PACS numbers: 43.30.Ft, 43.30.Re, 43.30.Pc [WMC] Pages: 2685–2697

I. INTRODUCTION

High-frequency acoustic scattering techniques are commonly used to obtain highly informative, though often qualitative, images of the biological and physical processes that occur in the ocean interior. For example, these techniques have been applied, with varying success, to the assessment of the distribution of zooplankton and fish (Holliday and Pieper, 1995; Medwin and Clay, 1998). It is also common to observe high-frequency acoustic scattering images of internal waves (Proni and Apel, 1975; Haury *et al.*, 1979; Farmer and Smith, 1979; Sandstrom *et al.*, 1989; Trevorrow, 1998; Farmer and Armi, 1999; Orr *et al.*, 2000). However, the exact interpretation of the scattering images in terms of a physical or biological process remains poorly understood. It is possible that the scattering arises from turbulent microstructure created by breaking internal waves, biological organisms or other particulates acting as passive tracers of the different physical processes, or, as is most likely, a combination of these processes.

In this paper we focus on the scattering of sound from turbulent oceanic microstructure. There is a significant body of evidence suggesting that high-frequency acoustic scattering from oceanic microstructure can be as strong as that due to zooplankton (Munk and Garrett, 1973; Proni and Apel, 1975; Goodman and Kemp, 1981; Thorpe and Brubaker, 1983; Goodman, 1990; Seim *et al.*, 1995; Seim, 1999). This observation has led to an interest in the possibility of using acoustic scattering techniques to remotely infer physical properties of the scattering medium. Such measurements could be valuable, for example, for the remote determination of fundamental ocean mixing parameters. The smallest length scales before mixing is complete, referred to as the microstructure scale, are set by molecular diffusion. Large gradients in the media properties can occur at these submillimeter to centimeter scales with the potential of creating measurable acoustic scattering returns. The acoustic wave lengths of interest are commensurate with the scale set by the physical process, corresponding to high-frequency sound spanning tens of kHz to a few MHz.

There are many alternative techniques for acquiring information regarding the physical and biological processes that occur in the ocean interior. However, most of these techniques are limited by either the volume sampled or the spatial and temporal resolution of the measurements. For example, free-falling vertical microstructure probes have extremely high spatial resolution, and yet are inherently one-dimensional in nature. The primary advantage of using acoustic techniques is the possibility of synoptically imaging large volumes of the ocean interior without compromising on the high spatial resolution of the measurements. The primary challenge involves the interpretation of the received signal in terms of relevant physical and biological parameters.

Accurate scattering models are key to the interpretation of the received acoustic signals. With such models, though typically also in conjunction with supporting physical and biological information, it may be possible to distinguish between the complex scattering signatures characteristic of dif-

[a]Electronic mail: alavery@whoi.edu

ferent physical and biological processes (Stanton *et al.*, 1994; Trevorrow, 1998). Under sufficiently well-characterized environments it may even be possible to infer properties of the processes that give rise to scattering (Lhermitte and Lemmin, 1993; Goodman *et al.*, 1992; Stanton *et al.*, 1994; Menemenlis and Farmer, 1995; Oeschger and Goodman, 1995). Of most interest to the current investigation, if the contribution from turbulent oceanic microstructure can be isolated, it may be possible to use scattering models to determine parameters such as the dissipation rates of turbulent kinetic energy or temperature variance.

Over the years a number of investigations have predicted that volume scattering resulting from fluctuations in oceanic temperature (arising from sound speed fluctuations alone) can be significant (Kraichnan, 1953; Munk and Garrett, 1973; Proni and Apel, 1975; Goodman and Kemp, 1981; Goodman, 1990). These predictions are supported by highly suggestive, though infrequently conclusive, evidence (Thorpe and Brubaker, 1983). More recently, it has been predicted that the effects of salinity fluctuations (again arising from sound speed fluctuations alone) can also be important (Seim *et al.*, 1995; Seim, 1999), particularly at higher frequencies and at locations where salinity plays a significant role in determining the vertical density stratification. To date though, acoustic scattering models specifically developed for turbulent oceanic microstructure have only included the effects of sound speed fluctuations, ignoring the effects of density fluctuations. Yet temperature and salinity microstructure gives rise to small scale fluctuations in both the sound speed and the density.

In this paper we show that under some circumstances it is critical to include the effects of density fluctuations to accurately predict acoustic scattering by turbulent oceanic microstructure. It has been common practice to consider fluctuations in the medium density in both the fields of medical ultrasound and atmospheric turbulence. The theory behind these seemingly disparate fields is broadly similar, though there are differences in the details of the application of the theory to the different fields (Chernov, 1960; Tatarski, 1961; Morse and Ingard, 1968; Ishimaru, 1978; Goodman and Kemp, 1981; Waag, 1984). The theory is based on far-field weak scattering for which the Born approximation can be used to evaluate the scattering cross section per unit volume, σ_v. However, unlike for medical ultrasound and atmospheric turbulence, the contribution to scattering from oceanic microstructure due to fluctuations in the density has typically been neglected. We have included the density contribution to σ_v for oceanic microstructure and have found that it can be comparable to the contribution from sound speed fluctuations, leading to increases in σ_v as large as a factor of 4 (corresponding to a 6-dB increase in the volume scattering strength), under certain conditions. In addition, the inclusion of density fluctuations leads to an expression for σ_v which contains an explicit dependence on the scattering angle.

This paper is organized as follows. In Sec. II, we derive an expression for σ_v that includes contributions from both density and sound speed fluctuations. Then, in Sec. III, by assuming a universal Batchelor spectrum for temperature and salinity, two expressions for σ_v are derived. One expression uses an upper bound for the temperature-salinity co-spectrum (Bendat and Piersol, 1986), and represents the case of a perfect correlation between temperature and salinity fluctuations. In addition, we have developed an expression for the co-spectrum that is based on Stern's theory (1968). In Sec. IV, general predictions for scattering from turbulent oceanic microstructure are made and the range of model input parameters for which the density contribution is important are isolated. We also make acoustic scattering predictions based on microstructure data obtained using a high resolution vertical microstructure profiler (Schmitt *et al.*, 1988). From these data, all the model parameters necessary for making scattering predictions at relevant scales can be determined. Finally, in Sec. V, the results are summarized and recommendations are made as to the conditions under which it is important to include the density term in predictions of acoustic scattering from oceanic microstructure.

II. SCATTERING FROM TURBULENT OCEANIC MICROSTRUCTURE

A general expression for the scattering cross section per unit volume, σ_v, due to random fluctuations in the compressibility and density of a weakly scattering medium is derived in Sec. II A. The resulting expression for σ_v is not specific to oceanic microstructure, and alternative derivations can be found in a number of standard text books (Chernov, 1960; Tatarski, 1961; Morse and Ingard, 1968; Ishimaru, 1978). In order to facilitate the application of this formulation to oceanic microstructure, the expression for σ_v in terms of the medium compressibility and density is then expressed in terms of the medium density and sound speed, though the expression that is derived is still not specific to oceanic microstructure, but holds for any weakly scattering random medium. Assumptions specific to oceanic microstructure are made in Sec. II B, where the temperature and salinity dependence of density and sound speed are explicitly included in the expression for σ_v.

A. Weak scattering by random media

A sound wave traveling through a region (of volume V) containing turbulent microstructure will be scattered from the changes in the medium density and compressibility. Suppose the density, $\rho(\mathbf{r},t)$, and compressibility, $\kappa(\mathbf{r},t)$, in the region fluctuate randomly in space and time, deviating from the average values of the medium density, ρ_0, and compressibility, κ_0. From this point on, we assume that the density and compressibility do not change significantly during the time of the measurement, and therefore that $\rho(\mathbf{r})$ and $\kappa(\mathbf{r})$ are time independent. Any temporal changes that might occur are simply considered as different realizations of the real random fields $\rho(\mathbf{r})$ and $\kappa(\mathbf{r})$. For a weakly scattering medium in which the fluctuations in the compressibility and density are small, such as that produced by turbulent microstructure, the Born approximation can be used. In this case, there are well known solutions to the wave equation, and the far field scattered pressure wave is given by (Morse and Ingard, 1968, p. 411, Eq. 8.1.14)

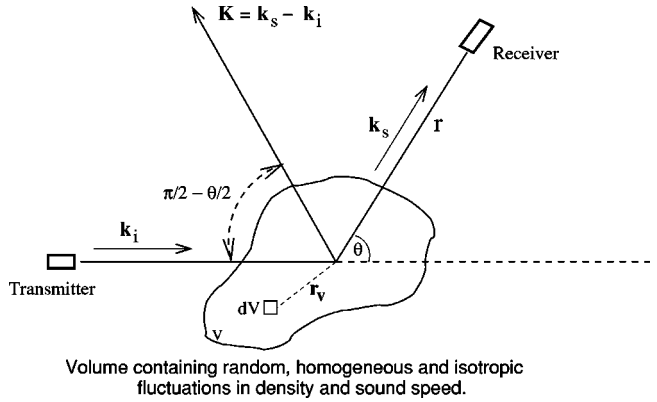

FIG. 1. Scattering geometry for an incident plane wave scattering from a bounded region of volume V containing random, stationary, homogeneous and isotropic fluctuations in the density and sound speed. $\mathbf{r}_v$ is the position vector of an infinitesimal volume element, $\hat{\mathbf{k}}_i$ is a unit vector along the direction of the incident wave, $\hat{\mathbf{k}}_s$ is a unit vector along the direction of the scattered wave, and $\mathbf{K}=k(\hat{\mathbf{k}}_s-\hat{\mathbf{k}}_i)$. The angle between the incident and scattered wave vectors is given by θ $(\hat{\mathbf{k}}_i\cdot\hat{\mathbf{k}}_s=\cos\theta)$, and $K=|\mathbf{K}|=2k\sin(\theta/2)$. K is maximum at backscattering where $\theta=\pi$.

$$p_s(r)=P_0\frac{e^{ikr}}{r}f, \tag{1}$$

where k is the incident acoustic wave number ($=2\pi/\lambda$, where λ is the acoustic wave length), r is the range from the scattering volume to the receiver, and P_0 is the incident acoustic pressure at some known reference range. The scattering amplitude, f, is a measure of the efficiency with which sound is scattered and is given by (Morse and Ingard, 1968, p. 413, Eq. 8.1.20):

$$f=\frac{k^2}{4\pi}\int_V \gamma(\mathbf{r}_v)e^{-i\mathbf{K}\cdot\mathbf{r}_v}d\mathbf{r}_v\,, \tag{2}$$

where

$$\gamma(\mathbf{r}_v)=\gamma_\kappa(\mathbf{r}_v)+\gamma_\rho(\mathbf{r}_v)\hat{\mathbf{k}}_i\cdot\hat{\mathbf{k}}_s=\gamma_\kappa(\mathbf{r}_v)+\gamma_\rho(\mathbf{r}_v)\cos\theta, \tag{3}$$

$\mathbf{r}_v$ is the position vector of any volume element relative to some arbitrary center point chosen within the volume V, $\hat{\mathbf{k}}_i$ is a unit vector along the direction of the incident wave, $\hat{\mathbf{k}}_s$ is a unit vector along the direction of the scattered wave, and $\mathbf{K}=k(\hat{\mathbf{k}}_s-\hat{\mathbf{k}}_i)$ (Fig. 1). The angle between the incident and scattered wave vectors is given by θ $(\hat{\mathbf{k}}_i\cdot\hat{\mathbf{k}}_s=\cos\theta)$, and $K=|\mathbf{K}|=2k\sin(\theta/2)$. The wave vector $\mathbf{K}$ is often referred to in the literature as the Bragg wave vector (Goodman, 1990). K is maximum at backscattering where $\theta=\pi$. The terms γ_κ and γ_ρ describe the variations in the medium compressibility and density and are given by (Morse and Ingard, 1968, p. 409, Eq. 8.1.11)

$$\gamma_\kappa=\frac{\kappa-\kappa_0}{\kappa_0}=\frac{c_0^2}{c^2}\frac{\rho_0}{\rho}-1 \quad\text{and}\quad \gamma_\rho=\frac{\rho-\rho_0}{\rho}=1-\frac{\rho_0}{\rho}, \tag{4}$$

where $c^2=1/\kappa\rho$ and c_0 is the mean sound speed. The contribution to scattering from fluid velocity has been ignored in the derivation of Eq. (2). This contribution has been investigated by others and, for oceanic microstructure, can be shown to be smaller than the other contributions by various orders of magnitude (Goodman, 1990). In fact, for backscattering, fluid velocity fluctuations do not contribute to scattering at all. It has also been assumed that the scattering volume is bounded and in the far field of both the transmitter and the receiver and that the transmitter and receiver are in the far field of the scattering volume.

The solution to the wave equation for bounded weakly scattering targets given by Eq. (2) has been used on many occasions as a starting point for developing scattering models for random media variability; it has been used for scattering of electromagnetic waves from atmospheric turbulence (Chernov, 1960; Tatarski, 1961; Morse and Ingard, 1968; Ishimaru, 1978), scattering of ultrasonic waves from different tissues in the field of medical ultrasound (Waag, 1984; Waag *et al.*, 1985, 1989), and it has also been used previously for scattering of high-frequency sound from temperature microstructure in the ocean (Munk and Garrett, 1973; Goodman and Kemp, 1981; Goodman, 1990). In addition, it has been used as a starting point for a number of acoustic scattering models for weakly scattering zooplankton (McGehee *et al.*, 1998; Stanton *et al.*, 1998; Chu and Ye, 1999; Lavery *et al.*, 2002). In contrast to the models developed for individual zooplankton, scattering from random media fluctuations is typically described in terms of the statistical properties of the medium. Thus, the scattering cross section per unit volume, σ_v, with units of inverse length, is given by (Ishimaru, 1978, p. 332, Eq. 16-10a)

$$\begin{aligned}\sigma_v&=\frac{r^2\langle p_s p_s^*\rangle}{VP_0^2}\\&=\frac{1}{V}\langle ff^*\rangle\\&=\frac{1}{V}\frac{k^4}{2^4\pi^2}\int_V\int_V B_\gamma(\mathbf{r}_1,\mathbf{r}_2)e^{-i\mathbf{K}\cdot(\mathbf{r}_1-\mathbf{r}_2)}d\mathbf{r}_1 d\mathbf{r}_2\,,\end{aligned} \tag{5}$$

where $\langle\ldots\rangle$ represents an ensemble average, and $\mathbf{r}_1$ and $\mathbf{r}_2$ are integration vectors over the volume V. The term $B_\gamma(\mathbf{r}_1,\mathbf{r}_2)\equiv\langle\gamma(\mathbf{r}_1)\gamma^*(\mathbf{r}_2)\rangle=\langle\gamma(\mathbf{r}_1)\gamma(\mathbf{r}_2)\rangle$ is the spatial correlation function of the real random field, γ, that describes the physical properties of the medium in the volume V. Note that the term volume scattering coefficient (denoted s_v) is more commonly used in the literature (instead of σ_v) when referring to an aggregation of discrete scatterers (Urick, 1980; Medwin and Clay, 1998).

Following the bulk of the published literature on scattering from turbulent microstructure we assume that the medium properties are homogeneous, meaning that the mean value of γ is constant and that the correlation function, $B_\gamma(\mathbf{r}_1,\mathbf{r}_2)$, does not change when the pair of points $(\mathbf{r}_1,\mathbf{r}_2)$ is displaced by the same amount in the same direction (Tatarski, 1961, p. 15). This latter assumption requires some justification since vertical stratification in the ocean is prevalent. However, the vertical stratification can be overturned by sufficiently large velocity shears. Typically, once overturning has occurred, physical structures that are aligned vertically or horizontally are destroyed, and the medium becomes turbulent, resulting in random homogeneous fluctuations in the

medium properties, at least locally within the scattering resolution volume. In the ocean interior the principal cause of mechanical mixing, or the source of high velocity shear resulting in overturning events and turbulent microstructure, is the presence of internal waves, which is where the assumptions we make here are most likely valid. Consequently, with the assumption that the fluctuations are locally homogeneous: $B_\gamma(\mathbf{r}_1,\mathbf{r}_2)=B_\gamma(\mathbf{r}_1-\mathbf{r}_2,0)=B_\gamma(\mathbf{r})$, where the substitution $\mathbf{r}=\mathbf{r}_1-\mathbf{r}_2$ has been made. Letting $\mathbf{x}=(\mathbf{r}_1+\mathbf{r}_2)/2$, and performing the integral over $\mathbf{x}$,

$$\sigma_v=\frac{k^4}{2^4\pi^2 V}\int_V\int_V B_\gamma(\mathbf{r})e^{-i\mathbf{K}\cdot\mathbf{r}}d\mathbf{r}d\mathbf{x}$$
$$=\frac{(\pi/2)\,k^4}{(2\pi)^3}\int_V B_\gamma(\mathbf{r})e^{-i\mathbf{K}\cdot\mathbf{r}}d\mathbf{r}. \tag{6}$$

For wave front curvature effects to be unimportant (Goodman, 1990; Waag *et al.*, 1985), there must be many characteristic length scales of the media variability encompassed within the first Fresnel radius, R_F. For a point transmitter and receiver, the first Fresnel radius refers to the locus of points for which the phase difference that arises from the path length difference between this locus of points and the center of the volume V is equal to $\pi/2$. At backscattering $R_F=\sqrt{R\lambda/2}$, where R is the range from the transmitter to the center of the volume V [an expression for R_F for forward scattering is given in Flatte *et al.* (1979, p. 91, Eq. 6.2.2)]. Next, we assume that the volume V is sufficiently large that many correlation lengths of the random media properties are encompassed by the volume. These assumptions allow the integral over the volume V in Eq. (6) to be converted to an integral over all space:

$$\sigma_v=\frac{(\pi/2)\,k^4}{(2\pi)^3}\int B_\gamma(\mathbf{r})e^{-i\mathbf{K}\cdot\mathbf{r}}d\mathbf{r}=\frac{\pi}{2}k^4\Phi(\mathbf{K}). \tag{7}$$

$\Phi(\mathbf{K})$ is the Fourier transform of the spatial correlation function of the medium variability, or simply the 3D wave number spectrum of the medium variability evaluated at $\mathbf{K}$. If we further assume that the medium is isotropic, then $B_\gamma(\mathbf{r})=B_\gamma(r)$ and $\Phi(\mathbf{K})=\Phi(K)$. The effects of anisotropy on scattering have been considered by Goodman (1990), who included a vertical wave number scaling factor, α (the ratio of vertical to horizontal spatial scale size), which resulted in an increase (α is typically <1) in the predicted scattering by a factor of α^{-2}. If the degree of anisotropy is small, the scattering cross section per unit volume is given by

$$\sigma_v=\frac{\pi}{2}k^4\Phi(K). \tag{8}$$

As mentioned earlier, a similar expression for σ_v can be found in a number of standard text books and has been used widely in the literature. However, when applied specifically to oceanic microstructure, the expression for B_γ inside the integral is typically given in terms of sound speed fluctuations alone, and the contribution from density fluctuations is ignored.

In order to facilitate the application of this formalism to the specific case of oceanic microstructure, we proceed to obtain an expression for σ_v which is explicitly written in terms of both density and sound speed fluctuations. This requires the evaluation of the spatial correlation function B_γ in terms of sound speed and density fluctuations. Since we are considering a weakly scattering medium, $\rho=\rho_0+\rho'$ and $c=c_0+c'$, where the inherent variations in the medium density, ρ', and sound speed, c', satisfy $c'/c_0\ll 1$ and $\rho'/\rho_0\ll 1$. From Eq. (4),

$$\gamma_\kappa=\left(1+\frac{c'}{c_0}\right)^{-2}\left(1+\frac{\rho'}{\rho_0}\right)^{-1}-1\approx -2\frac{c'}{c_0}-\frac{\rho'}{\rho_0}$$

and

$$\gamma_\rho=\frac{\rho'}{\rho_0}\left(1+\frac{\rho'}{\rho_0}\right)^{-1}\approx\frac{\rho'}{\rho_0}, \tag{9}$$

where only first order terms in the primed variables have been kept. Making use of these relationships, the trigonometric relationship $(1-\cos\theta)=2\sin^2(\theta/2)$, as well as the definition of γ [Eq. (3)], the spatial correlation function of media variability becomes

$$B_\gamma(r)=4\left(\left\langle\frac{c'}{c_0}\frac{c'^*}{c_0}\right\rangle+2\sin^2\left(\frac{\theta}{2}\right)\left\langle\frac{c'}{c_0}\frac{\rho'^*}{\rho_0}\right\rangle\right.$$
$$\left.+\sin^4\left(\frac{\theta}{2}\right)\left\langle\frac{\rho'}{\rho_0}\frac{\rho'^*}{\rho_0}\right\rangle\right). \tag{10}$$

Using this expression for B_γ, σ_v [Eq. (8)] becomes

$$\sigma_v=2\pi k^4\left(\Phi_c(K)+2\sin^2\left(\frac{\theta}{2}\right)\Phi_{c\rho}(K)\right.$$
$$\left.+\sin^4\left(\frac{\theta}{2}\right)\Phi_\rho(K)\right), \tag{11}$$

where $\Phi_c(K)$, $\Phi_\rho(K)$, and $\Phi_{c\rho}(K)$ are the 3D wave number spectra of the sound speed fluctuations, density fluctuations, and the correlation between sound speed and density fluctuations. In arriving at this expression, it should be noted that all cross-terms between density and sound speed fluctuations have been included.

No assumptions specific to scattering from oceanic microstructure have been made in deriving this general expression, which holds (theoretically) for any weakly scattering random medium. To date, various equivalent forms of Eq. (11) have been used to describe scattering by atmospheric turbulence and organ tissues. However, all formulations specific to scattering from oceanic microstructure have only included fluctuations in the sound speed, resulting in simply the first term in this expression. The inclusion of density fluctuations results in two extra terms, both of which have an explicit angular dependence. It is clear from the wave equation where this angular dependence arises since the term involving density depends on the *gradient* of the density. We turn now to the specific case of scattering from turbulent oceanic microstructure.

B. Application to turbulent oceanic microstructure

The most convenient parameters for describing scattering from turbulent oceanic microstructure are temperature

TABLE I. The following parameters were used for the prediction of acoustic scattering from oceanic microstructure (Flatte *et al.*, 1979: p. 5, Eq. 1.1.6): $a=3.19\times10^{-3}$ ($^\circ C^{-1}$), $b=0.96\times10^{-3}$ (psu^{-1}), $\alpha=0.13\times10^{-3}$ ($^\circ C^{-1}$), $\beta=0.8\times10^{-3}$ (psu^{-1}), $\nu=0.15\times10^{-5}$ ($m^2\,s^{-1}$), $D_T=1.38\times10^{-7}$ ($m^2\,s^{-1}$), $D_S=0.95\times10^{-9}$ ($m^2\,s^{-1}$), and $L_e=145.26$. Modest values of ϵ (1×10^{-8} W kg^{-1}) and χ_T ($1\times10^{-6}\,^\circ C^2\,s^{-1}$) were chosen, giving values of $k^*=29$ (cpm), $k_d=769$ (cpm), and $k_{ds}=9207$ (cpm). Acoustic frequencies ranging from approximately 10 kHz ($k=42$ cpm, $\lambda=15$ cm) to 2 MHz ($k=8379$ cpm, $\lambda=0.75$ mm) were used to make the scattering predictions. Based on these parameters, most of the predictions lie in the viscous-convective range, where $k>k^*$. The following three cases were investigated (all parameters dimensionless unless otherwise stated). Note that the values for $R_{\rho c}$ in this table were evaluated at backscattering ($\theta=\pi$).

Case no.	$R_{\rho c}$	$R_{\rho c}^{-1}$	R_c	R_ρ	$\delta(^\circ C\,psu^{-1})$	$R_{\rho c}/L_e$ ($\times10^{-2}$)	$\frac{\max(\sigma_v^S)}{\max(\sigma_v^T)}$ [Eq. (34)]
1	1	1	1.911	0.094	0.575	0.6	10
2	3.477	0.288	6.646	0.325	2	2.39	0.72
3	0.165	0.287	0.548	0.0268	3.49	0.20	367.3

and salinity, since these are the most commonly measured, and consequently better mapped and understood oceanographic parameters. The aim of this section is to express Eq. (11) in terms of the wave number spectra of temperature and salinity, instead of density and sound speed. Fluctuations in the sound speed and density are related to the small scale fluctuations in temperature, T', and salinity, S', by

$$\frac{c'}{c_0}=\frac{1}{c_0}\frac{\partial c}{\partial T}T'+\frac{1}{c_0}\frac{\partial c}{\partial S}S'=aT'+bS', \tag{12}$$

where

$$a\equiv\frac{1}{c_0}\frac{\partial c}{\partial T}\quad\text{and}\quad b\equiv\frac{1}{c_0}\frac{\partial c}{\partial S}, \tag{13}$$

and

$$\frac{\rho'}{\rho_0}=\frac{1}{\rho_0}\frac{\partial \rho}{\partial T}T'+\frac{1}{\rho_0}\frac{\partial \rho}{\partial S}S'=-\alpha T'+\beta S', \tag{14}$$

where

$$\alpha\equiv-\frac{1}{\rho_0}\frac{\partial \rho}{\partial T}\quad\text{and}\quad \beta\equiv\frac{1}{\rho_0}\frac{\partial \rho}{\partial S}. \tag{15}$$

Here α is the coefficient of thermal expansion and β is the coefficient for saline contraction. The importance of salinity versus temperature in determining scattering from sound speed and density variations can be gauged by examining the vertical changes in sound speed and density,

$$\frac{1}{c_0}\frac{dc}{dz}=a\frac{\partial T}{\partial z}+b\frac{\partial S}{\partial z}\quad\text{and}\quad\frac{1}{\rho_0}\frac{d\rho}{dz}=-\alpha\frac{\partial T}{\partial z}+\beta\frac{\partial S}{\partial z}, \tag{16}$$

and forming the sound speed and density ratios:

$$R_c\equiv\frac{a}{b}\delta\quad\text{and}\quad R_\rho\equiv\frac{\alpha}{\beta}\delta,\quad\text{where}\quad\delta=\frac{\partial T/\partial z}{\partial S/\partial z}. \tag{17}$$

Here R_c and R_ρ indicate the relative importance of temperature versus salinity in determining the vertical sound speed and density gradients, and play a critical role in determining the contribution to scattering from salinity relative to temperature. If $-1<R_c<1$, then salinity plays a more dominant role than temperature in determining vertical sound speed variations. If $-1<R_\rho<1$, salinity plays a more dominant role than temperature in determining vertical density variations. Typical values of these parameters for an open ocean environment are given in Table I. From these values, $R_c=3.32\ \delta$ and $R_\rho=0.16\ \delta$. There is typically larger variability in the parameter δ than in a, b, α, or β. However, it can be seen that the range of values of δ ($-6.25<\delta<6.25$) for which $-1<R_\rho<1$ is significantly wider than the range of values of δ ($-0.30<\delta<0.30$) for which $-1<R_c<1$. In addition, in order to assess the importance of including fluctuations in the density when calculating acoustic scattering from turbulent oceanic microstructure, it is necessary to compare the fractional change in the sound speed from salinity, b, and the coefficient of haline contraction, β. Since these terms are approximately equal, we conclude that it is important to include the contribution to scattering from density fluctuations.

In order to evaluate σ_v in terms of temperature and salinity fluctuations, it is necessary to evaluate B_γ in terms of T' and S'. Making use of Eqs. (10), (12), and (14),

$$B_\gamma(r)=4[A^2\langle T'T'^*\rangle+B^2\langle S'S'^*\rangle+2AB\langle T'S'^*\rangle], \tag{18}$$

where

$$A=a-\alpha\sin^2\left(\frac{\theta}{2}\right)\quad\text{and}\quad B=b+\beta\sin^2\left(\frac{\theta}{2}\right). \tag{19}$$

Using this expression for B_γ, σ_v becomes

$$\sigma_v=2\pi k^4(A^2\Phi_T(K)+B^2\Phi_S(K)+2AB\Phi_{ST}(K)), \tag{20}$$

where $\Phi_T(K)$, $\Phi_S(K)$, and $\Phi_{ST}(K)$ are the 3D wave number spectra of temperature, salinity, and the temperature-salinity co-spectrum, all evaluated at the wave number K.

This is a general expression for the scattering cross section per unit volume describing scattering from stationary, homogeneous, and isotropic turbulent oceanic microstructure. Unlike previous formulations of scattering specific to turbulent oceanic microstructure, which only included fluctuations in the sound speed, the scattering cross section per unit volume derived here also includes the contributions from variability in the density. It has typically been assumed (Tatarski, 1961; Goodman and Kemp, 1981; Thorpe and Brubaker, 1983; Goodman, 1990; Seim *et al.*, 1995; Seim, 1999) that scattering from oceanic microstructure is dominated by sound speed fluctuations, that is, $\rho'/\rho_0\ll c'/c_0$. In

this case it follows from Eq. (9) that $\gamma_\kappa \approx -2c'/c_0 = -2aT'$ and $\gamma_\rho \approx 0$. If the effects of salinity are ignored, this is a reasonable assumption since for typical open ocean environments $\alpha/a \approx 0.03$. As a result, $\sigma_v = 2\pi k^4 a^2 \Phi_T(K)$, which is the first term of Eq. (20) with the coefficient A replaced by a. Seim *et al.* (1995) developed this theory one step further, and included the contributions to scattering from fluctuations in the sound speed originating from both temperature and salinity microstructure. In this scenario, $\gamma_\rho = \rho'/\rho_0 \approx 0$, $\gamma_\kappa \approx -2c'/c_0 = -2(aT' + bS')$, and the scattering cross section per unit volume is given by

$$\sigma_v = 2\pi k^4 (a^2 \Phi_T(K) + b^2 \Phi_S(K) + 2ab\Phi_{ST}(K)). \quad (21)$$

This expression is identical in form to Eq. (20) with the coefficient A replaced by a, and B replaced by b. However, the coefficients A and B contain terms involving the coefficient of thermal contraction (α), the coefficient of haline expansion (β), and the bi-static scattering angle (θ) that are specific to the inclusion of density fluctuations. It can be seen from the expressions for A and B that the contribution to scattering from the density term is maximum at backscatter ($\theta = \pi$) and disappears at angles close to forward scattering ($\theta = 0$). Finally, it should be noted that since $\alpha \gg a$ while $\beta \approx b$, the contribution to scattering from density fluctuations will be most significant under conditions in which salinity (and not temperature) microstructure dominates the scattering.

For homogeneous and isotropic random media fluctuations, the 3D wave number spectrum $\Phi(K)$ can be related to the 1D wave number spectrum, $\phi(K)$ (Tatarski, 1961, p.17, Eq. 1.27) by

$$\Phi(K) = \left[-\frac{1}{2\pi k} \frac{d\phi(k)}{dk} \right]_K. \quad (22)$$

Expressing σ_v in terms of 1D wave number spectra is useful as standard oceanographic measurements typically involve performing vertical temperature and conductivity profiles, resulting in 1D wave number spectra. Applying Eq. (22) to Eq. (20), σ_v is given by

$$\begin{aligned} \sigma_v &= -k^4 \left[\frac{1}{k} \frac{d}{dk} (A^2 \phi_T(k) + B^2 \phi_S(k) + 2AB\phi_{ST}(k)) \right]_K \\ &= -\frac{k^4}{K} \left(A^2 \frac{d\phi_T(K)}{dk} + B^2 \frac{d\phi_S(K)}{dk} + 2AB \frac{d\phi_{ST}(K)}{dk} \right), \end{aligned} \quad (23)$$

where the contribution to scattering from temperature fluctuations alone, σ_v^T, is given by the first term in this expression, scattering from salinity fluctuations alone, σ_v^S, is given by the second term in this expression, and the scattering from the temperature-salinity co-spectrum alone, σ_v^{ST}, is given by the last term. Using these expressions, it may ultimately be possible to measure the acoustic scattering from turbulent oceanic microstructure and invert for the wave number spectra of temperature and salinity, and their co-spectrum. Thus, using high-frequency acoustic scattering techniques, it may be possible to (1) overcome the technical difficulties associated with resolving the salinity spectrum with standard oceanographic measurement techniques, and (2) obtain an estimate for the yet unmeasured temperature-salinity co-spectrum.

III. PARAMETRIZATION OF SCATTERING IN TERMS OF MEASURABLE PHYSICAL PARAMETERS

The 1D wave number spectra of temperature, salinity, and the co-spectrum must be expressed in terms of measurable physical parameters in order to predict acoustic scattering from turbulent oceanic microstructure. In this section we derive expressions for σ_v^T and σ_v^S based on wave number spectra for temperature and salinity similar to those proposed by Batchelor (1959). In addition, two models for the co-spectrum of temperature and salinity are used to calculate σ_v^{ST}.

A. The temperature and salinity spectra

As suggested by Seim *et al.* (1995, 1999), we use an inertial-convective model for spatial wave numbers smaller than $k^* = (1/2^3)(\epsilon/\nu^3)^{1/4}$, and a viscous-convective model at higher wave numbers, where ν ($\mathrm{m^2 s^{-1}}$) is the molecular viscosity, and ϵ ($\mathrm{W\,kg^{-1}}$) is the dissipation rate of turbulent kinetic energy. Within the framework of these models, the temperature spectrum (Batchelor, 1959; Dillon and Caldwell, 1980) is given by

$$\begin{aligned} \phi_T^<(\tilde{k}) &= A^* \chi_T \epsilon^{-1/3} \tilde{k}^{-5/3} \quad \text{for } \tilde{k} \leqslant k^*, \\ \phi_T^>(\tilde{k}) &= \frac{\chi_T}{\zeta} \frac{G(\xi_T)}{\tilde{k}} \quad \text{for } \tilde{k} \geqslant k^*, \end{aligned} \quad (24)$$

where $\zeta = (\epsilon/\nu)^{1/2}/q$ is the strain rate. The spatial wave number is denoted by $\tilde{k}$ to distinguish it from the acoustic wave number k. Throughout the remainder of this paper, superscripts $^<$ and $^>$ indicate that the quantity being referred to is valid for wave numbers smaller than, and larger than, k^*, respectively. The salinity spectrum is given by

$$\begin{aligned} \phi_S^<(\tilde{k}) &= A^* \chi_S \epsilon^{-1/3} \tilde{k}^{-5/3} \quad \text{for } \tilde{k} \leqslant k^*, \\ \phi_S^>(\tilde{k}) &= \frac{\chi_S}{\zeta} \frac{G(\xi_S)}{\tilde{k}} \quad \text{for } \tilde{k} \geqslant k^*. \end{aligned} \quad (25)$$

The dimensionless function $G(\xi)$ (valid for either ξ_T or ξ_S) is defined by

$$G(\xi) \equiv e^{-\xi^2/2} - \xi \int_\xi^\infty e^{-x^2/2} dx, \quad (26)$$

where $\xi_T = \sqrt{2q}\tilde{k}/k_d$ and $\xi_S = \sqrt{2q}\tilde{k}/k_{ds}$ are dimensionless wave numbers, $k_d = (\epsilon/\nu D_T^2)^{1/4}$ is the diffusive cutoff wave number for temperature, $k_{ds} = (\epsilon/\nu D_S^2)^{1/4}$ is the diffusive cutoff wave number for salt, D_T ($\mathrm{m^2 s^{-1}}$) is the molecular diffusivity for temperature, and D_S ($\mathrm{m^2 s^{-1}}$) is the molecular diffusivity for salt. A^* and q are constants: $A^* = 0.925$ is chosen such that the spectra are equal at k^* (Dillon and Caldwell, 1980), and $q = 3.7$ (Oakey, 1982). The dissipation rates of salt and temperature variance are given by χ_S

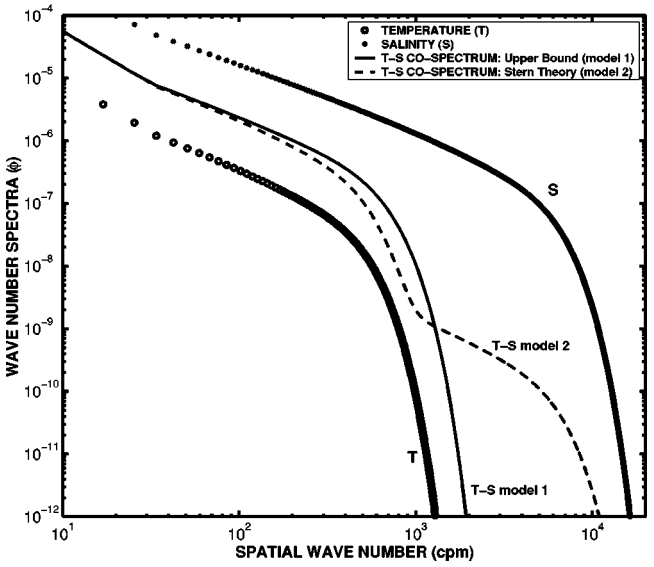

FIG. 2. Estimated wave number spectra (based on parameters for case 3 in Table I) as a function of spatial wave number for temperature (open circles), ϕ_T; salinity (crosses), ϕ_S; and the temperature-salinity co-spectrum, ϕ_{ST} (solid and dashed lines). Two models have been used for the co-spectrum: the first is an upper bound for co-spectrum (solid line), representing perfect positive correlation between temperature and salinity fluctuations, while the second model for the co-spectrum (dashed line) we have derived.

($\mathrm{psu}^2\mathrm{s}^{-1}$) and χ_T ($^\circ\mathrm{C}^2\mathrm{s}^{-1}$), respectively. Typical values of these parameters are given in Table I.

Since the parametrization of the temperature and salinity spectra are identical, the only difference between these spectra is the relevant scale set by k_d and k_{ds}, and the overall magnitude of the spectra, which is determined to a large part by χ_T and χ_S (Fig. 2). Since χ_S remains unmeasured, it is assumed that temperature and salinity have equal eddy diffusivities, from which it follows that the scalar dissipation rates are related by $\chi_S = \chi_T/\delta^2$ (Osborn and Cox, 1972; Gregg, 1984). The roll-off for the salinity spectrum occurs at higher spatial wave numbers ($\sim$ a factor of 10) than the roll-off for the temperature spectrum since the molecular diffusivity for salt is approximately two orders of magnitude smaller than the molecular diffusivity for temperature.

In order to evaluate σ_v it is necessary to calculate terms such as $d\phi_T/d\tilde{k}$ and $d\phi_S/d\tilde{k}$. For $\tilde{k} \leqslant k^*$,

$$\frac{d\phi_T^<(\tilde{k})}{d\tilde{k}} = -\frac{5}{3}\frac{\phi_T^<(\tilde{k})}{\tilde{k}} = -\frac{5}{3}\chi_T \epsilon^{-1/3}\tilde{k}^{-8/3},$$
$$\frac{d\phi_S^<(\tilde{k})}{d\tilde{k}} = -\frac{5}{3}\frac{\phi_S^<(\tilde{k})}{\tilde{k}} = -\frac{5}{3}\chi_S \epsilon^{-1/3}\tilde{k}^{-8/3}, \tag{27}$$

while for $\tilde{k} \geqslant k^*$,

$$\frac{d\phi_T^>(\tilde{k})}{d\tilde{k}} = -\frac{\phi_T^>(\tilde{k})}{\tilde{k}}\frac{e^{-\xi_T^2/2}}{G(\xi_T)} = -\frac{\chi_T}{\zeta}\frac{e^{-\xi_T^2/2}}{\tilde{k}^2},$$
$$\frac{d\phi_S^>(\tilde{k})}{d\tilde{k}} = -\frac{\phi_S^>(\tilde{k})}{\tilde{k}}\frac{e^{-\xi_S^2/2}}{G(\xi_S)} = -\frac{\chi_S}{\zeta}\frac{e^{-\xi_S^2/2}}{\tilde{k}^2}. \tag{28}$$

A quantity which will be useful later is the ratio of ϕ_S to ϕ_T:

$$\left(\frac{\phi_S^<(\tilde{k})}{\phi_T^<(\tilde{k})}\right)^{1/2} = \left(\frac{\chi_S}{\chi_T}\right)^{1/2} \equiv \frac{1}{\delta} \quad \text{for } \tilde{k} \leqslant k^*,$$
$$\left(\frac{\phi_S^>(\tilde{k})}{\phi_T^>(\tilde{k})}\right)^{1/2} = \left(\frac{\chi_S}{\chi_T}\frac{G(\xi_S)}{G(\xi_T)}\right)^{1/2} = \frac{R_G}{\delta} \quad \text{for } \tilde{k} \geqslant k^*, \tag{29}$$

where $R_G \equiv (G(\xi_S)/G(\xi_T))^{1/2}$. At low wave numbers $R_G \approx 1$, while above the diffusive cutoff wave number for heat, R_G increases rapidly, and the temperature spectrum is much smaller than the salinity spectrum, though both may be small.

It is now possible to evaluate σ_v^T and σ_v^S, recalling that the wave number spectra must be evaluated at the wave number, K, which is related to the acoustic wave number, k, by $K = 2k\sin(\theta/2)$:

$$\sigma_v^{T<} = -A^2\left(\frac{k^4}{K}\right)\left[\frac{d\phi_T^<(\tilde{k})}{d\tilde{k}}\right]_K = A^2\left(\frac{k^4}{K}\right)\left(\frac{5}{3}\frac{\phi_T^<(K)}{K}\right),$$
$$\sigma_v^{T>} = -A^2\left(\frac{k^4}{K}\right)\left[\frac{d\phi_T^>(\tilde{k})}{d\tilde{k}}\right]_K = A^2\left(\frac{k^4}{K}\right)\left(\frac{e^{-\xi_T^2/2}}{G(\xi_T)}\frac{\phi_T^>(K)}{K}\right), \tag{30}$$

and

$$\sigma_v^{S<} = -B^2\left(\frac{k^4}{K}\right)\left[\frac{d\phi_S^<(\tilde{k})}{d\tilde{k}}\right]_K = B^2\left(\frac{k^4}{K}\right)\left(\frac{5}{3}\frac{\phi_S^<(K)}{K}\right),$$
$$\sigma_v^{S>} = -B^2\left(\frac{k^4}{K}\right)\left[\frac{d\phi_S^>(\tilde{k})}{d\tilde{k}}\right]_K = B^2\left(\frac{k^4}{K}\right)\left(\frac{e^{-\xi_S^2/2}}{G(\xi_S)}\frac{\phi_S^>(K)}{K}\right). \tag{31}$$

Using Eqs. (30) and (31), the ratio of the temperature to salinity contribution to scattering is given by

$$\frac{\sigma_v^{T<}}{\sigma_v^{S<}} = \frac{A^2}{B^2}\frac{\phi_T^<(K)}{\phi_S^<(K)} = \delta^2\frac{A^2}{B^2} = R_{\rho c}^2 \quad \text{for } \tilde{k} \leqslant k^*,$$
$$\frac{\sigma_v^{T>}}{\sigma_v^{S>}} = \delta^2\frac{A^2}{B^2}e^{-(\xi_T^2-\xi_S^2)/2} = R_{\rho c}^2 e^{-(\xi_T^2-\xi_S^2)/2} \quad \text{for } \tilde{k} \geqslant k^*. \tag{32}$$

Here $R_{\rho c}$ is defined by

$$R_{\rho c} \equiv \delta \frac{A}{B} = \delta \frac{(a - \alpha \sin^2(\theta/2))}{(b + \beta \sin^2(\theta/2))}$$

$$= R_c \frac{(1 - (\alpha/a)\sin^2(\theta/2))}{(1 + (\beta/b)\sin^2(\theta/2))}. \quad (33)$$

The definition of $R_{\rho c}$ parallels the definitions for the vertical density, R_ρ, and sound speed, R_c, ratios [Eq. (17)]. $R_{\rho c}$ expresses the relative importance of temperature versus salinity in determining the vertical gradient for a combined density and sound speed expression. $R_{\rho c}$ depends on the multi-static scattering angle, but is independent of the acoustic wave number. For a particular set of (α, β, δ, a, b) values, $R_{\rho c}$ changes by approximately a factor 2 as a function of angle, decreasing from R_c at $\theta = 0°$ (forward scattering) to approximately $R_c/2$ at $\theta = 180°$ (backscattering). The reason for this is that for typical open ocean parameters, $\alpha \ll a$, and $(1 - \alpha/a) \approx 1$, while $\beta \approx b$, and $(1 + \beta/b) \approx 2$.

Finally, it is straightforward to show that the maximum value of σ_v^T occurs at a wave number corresponding to $k_d(2q)^{-1/2}$ (subject to the condition that $k^* < k_d$), while the maximum value of σ_v^S occurs at $k_{ds}(2q)^{-1/2}$. The ratio of the maximum value of σ_v^T to the maximum value in σ_v^S is given by

$$\frac{\max(\sigma_v^T)}{\max(\sigma_v^S)} = R_{\rho c}^2 \left(\frac{k_d}{k_{ds}} \right) = R_{\rho c}^2 \left(\frac{D_S}{D_T} \right)^{1/2} \approx \frac{R_{\rho c}^2}{10}. \quad (34)$$

B. The temperature and salinity co-spectrum

Currently, there are no data regarding the co-spectrum of temperature and salinity, and the existing theory is based on limiting cases, such as perfect correlation between temperature and salinity, or no correlation at all. We make predictions based on two models for the co-spectrum. The first involves an upper bound for the co-spectrum (Bendat and Piersol, 1986), representing a perfect correlation between temperature and salinity fluctuations. This upper bound for the co-spectrum has been used previously by other authors (Washburn *et al.*, 1996; Seim, 1999). The second model for the co-spectrum we have derived and it is based on the temperature-salinity co-variance theory of Stern (1968). It should be noted that a zero-correlation model can be implemented by neglecting the contribution to scattering from the co-spectrum term.

1. Model 1: Upper bound

The upper bound for the temperature and salinity co-spectrum is given by (Bendat and Piersol, 1986, p. 117, Eq. 5.11) $\phi_{ST}(\tilde{k}) = (\phi_T(\tilde{k})\phi_S(\tilde{k}))^{1/2}$. To evaluate σ_v^{ST} using this model for the co-spectrum it is necessary to first evaluate $d\phi_{ST}/d\tilde{k}$:

$$\frac{d\phi_{ST}}{d\tilde{k}} = \frac{1}{2} \left(\frac{\phi_S}{\phi_T} \right)^{1/2} \frac{d\phi_T}{d\tilde{k}} + \frac{1}{2} \left(\frac{\phi_S}{\phi_T} \right)^{-1/2} \frac{d\phi_S}{d\tilde{k}}, \quad (35)$$

where $d\phi_T/d\tilde{k}$ and $d\phi_S/d\tilde{k}$ are given by Eqs. (27) and (28). From Eq. (23), for $\tilde{k} < k^*$,

$$\sigma_v^{ST<} = -2AB \left(\frac{k^4}{K} \right) \frac{d\phi_{ST}^<}{dk}$$

$$= \frac{B}{A} \frac{1}{\delta} \sigma_v^{T<} + \frac{A}{B} \delta \sigma_v^{S<}$$

$$= \frac{1}{R_{\rho c}} \sigma_v^{T<} + R_{\rho c} \sigma_v^{S<}, \quad (36)$$

and, for wave numbers above k^*,

$$\sigma_v^{ST>} = -2AB \left(\frac{k^4}{K} \right) \frac{d\phi_{ST}^>}{dk}$$

$$= \frac{B}{A} \frac{R_G}{\delta} \sigma_v^{T>} + \frac{A}{B} \frac{\delta}{R_G} \sigma_v^{S>}$$

$$= \frac{R_G}{R_{\rho c}} \sigma_v^{T>} + \frac{R_{\rho c}}{R_G} \sigma_v^{S>}. \quad (37)$$

2. Model 2: Co-spectrum based on Stern's theory

We have developed a model for the co-spectrum that is based on Stern's theory (1968). Batchelor spectra for T and S are used in this derivation to evaluate the variances as a function of wave number, and we assume that this model is valid for all wave numbers of interest here. Our co-spectrum model is given by

$$\phi_{ST}(\tilde{k}) = \frac{\phi_T(\tilde{k})}{\delta} + \frac{\delta}{L_e} \phi_S(\tilde{k}), \quad (38)$$

where L_e ($= D_T/D_S$) is the diffusivity ratio, or Lewis number, and varies from ≈ 80 in warm water to ≈ 230 in cold water. It can be seen from Fig. 2 that at high spatial wave numbers our co-spectrum model predicts a higher correlation between temperature and salinity fluctuations than the upper bound model.

The scattering contribution from this co-spectrum model is given by

$$\sigma_v^{ST} = -2AB \left(\frac{k^4}{K} \right) \frac{d\phi_{ST}(K)}{d\tilde{k}}$$

$$= \frac{2}{\delta} \frac{B}{A} \sigma_v^T + 2 \frac{\delta}{L_e} \frac{A}{B} \sigma_v^S$$

$$= \frac{2}{R_{\rho c}} \sigma_v^T + \frac{2R_{\rho c}}{L_e} \sigma_v^S. \quad (39)$$

Since the sign of $R_{\rho c}$ is determined by δ, and all terms relating to the co-spectrum contribution to scattering have $R_{\rho c}$ or $R_{\rho c}^{-1}$ as a prefactor, the effect of the co-spectrum on σ_v is determined by the sign of δ. If δ is positive, either model for the co-spectrum results in an increase in the magnitude of σ_v: $\sigma_v \geqslant \sigma_v^S + \sigma_v^T$. If δ is negative, $\sigma_v \leqslant \sigma_v^S + \sigma_v^T$.

IV. PREDICTIONS

To illustrate many of the points of this paper, values that are typical for an open ocean environment were chosen for the model input parameters (Table I). Modest values of ϵ and

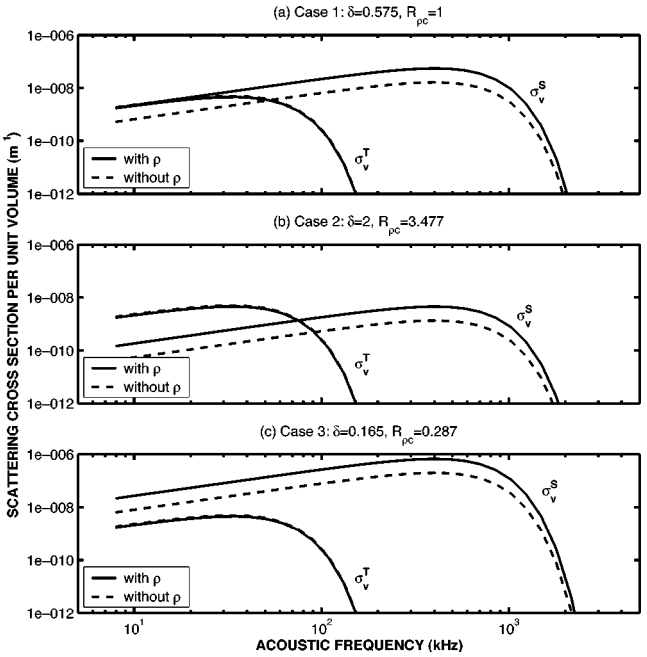

FIG. 3. The temperature, σ_v^T, and salinity, σ_v^S, contributions to the scattering cross section per unit volume as a function of acoustic frequency (at backscattering) for model input parameters given in Table I. The solid lines correspond to σ_v^T and σ_v^S calculated with the density fluctuations included, while the dashed lines correspond to σ_v^T and σ_v^S calculated without the inclusion of density fluctuations. The inclusion of density fluctuations does not significantly affect the value of σ_v^T at any frequency or angle. In contrast, inclusion of the density term significantly increases the value of σ_v^S over the entire frequency range investigated. The *relative* increase in scattering that occurs due to the inclusion of density fluctuations does not depend on the values of ϵ and χ_T. Thus the importance of including the density term can be assessed without precise knowledge of the dissipation rates.

χ_T were chosen. Changes in χ_T simply result in an overall increase or decrease in σ_v, and do not change the overall shape of σ_v. On the other hand, changes in ϵ affect both the overall magnitude as well as the wave number dependence of σ_v. Since the parameter $R_{\rho c}$ is important in determining the relative magnitudes of the temperature and salinity contributions to scattering, and thus is also important in determining the relative importance of the density versus sound speed contribution, predictions based on three values of $R_{\rho c}$, evaluated at $\theta=\pi$, are discussed in this section (Table I): (1) $R_{\rho c}=1$, (2) $R_{\rho c}=3.477(>1)$, and (3) $R_{\rho c}=0.287(<1)$. We assume a backscattering orientation for most of the predictions presented in this section, though the angular dependence is also investigated in Sec. IV D.

A. The relative contribution to scattering from density versus sound speed fluctuations

The importance of including density fluctuations in predicting scattering from turbulent oceanic microstructure can be assessed by comparing predictions of σ_v arising from the inclusion of both sound speed and density fluctuations [Eq. (20)] to predictions of σ_v arising from the inclusion of sound speed fluctuations alone [Eq. (21)] (Fig. 3). The expressions for σ_v are very similar in form: the coefficients A and B in Eq. (20) are simply replaced by a and b in Eq. (21). Since $a \gg \alpha$, and $A=a-\alpha\sin^2(\theta/2)\approx a$, the inclusion of the density term has a minimal effect on σ_v^T, at any angle. In contrast, since $b\approx\beta$, and $B=b+\beta\sin^2(\theta/2)$, the inclusion of the density term increases σ_v^S from b^2 to $B^2\approx 4b^2$ at backscattering. This corresponds to approximately a 6-dB increase in the scattering level. The magnitude of σ_v^{ST} increases from $2ab$ to $2AB\approx 4ab$ due to the inclusion of the density term, corresponding to a 3-dB increase. These *relative* increases do not depend strongly on the model input parameter values, the form of the spectra or co-spectrum, or on the acoustic wave number (at any given scattering angle). However, the effects of including density fluctuations are strongly dependent on the scattering angle, with the largest effects occurring at backscattering, while becoming negligible at angles close to forward scattering. From this point on, all predictions will include the contribution to scattering from density fluctuations.

B. The relative contribution to scattering from temperature versus salinity microstructure

The relative magnitude of σ_v^T and σ_v^S is strongly dependent on the spatial wave number (Fig. 3), which is related to the acoustic wave number through the condition that $K=2k\sin(\theta/2)$. For spatial wave numbers below k^*, the term $R_{\rho c}^2$ determines the relative magnitude of σ_v^T and σ_v^S [Eq. (32)]. Since $R_{\rho c}^2$ is independent of wave number, at any given scattering angle, σ_v^T and σ_v^S are simply offset by a constant amount: if $|R_{\rho c}|>1$, then σ_v^T dominates, while if $|R_{\rho c}|<1$, then σ_v^S dominates the scattering. For spatial wave numbers above k^*, the term $R_{\rho c}^2 e^{-(\xi_T^2-\xi_S^2)/2}$, which is a function of both angle and wave number, determines the relative magnitude of σ_v^T and σ_v^S [Eq. (32)]. Above the diffusive cutoff wave number for temperature, k_d, the exponential term decays rapidly and, for any reasonable value of $R_{\rho c}^2$, $\sigma_v^S \gg \sigma_v^T$ (though both may be small). For wave numbers between k^* and k_d, the exponential term does not yet deviate greatly from 1, and $R_{\rho c}^2$ is again critical in determining the relative magnitude of σ_v^T and σ_v^S. A more general way to estimate the importance of salinity versus temperature in determining scattering is to examine the maximum values attained by σ_v^S and σ_v^T [Eq. (34)]. The maximum value of σ_v^S is larger than the maximum value of σ_v^T when $R_{\rho c}<(D_T/D_S)^{1/4}\approx 3$, though it must be recalled that these maxima occur at different wave numbers since the diffusive cutoff wave numbers for heat and salt differ by an order of magnitude.

C. The relative contribution to scattering from the co-spectrum

The contribution to scattering from the upper bound co-spectrum (model 1) is given by Eq. (36) for spatial wave numbers below k^* and by Eq. (37) for spatial wave numbers above k^* (Fig. 4). Recalling that $\sigma_v^{T<}=R_{\rho c}^2\sigma_v^{S<}$ [Eq. (32)], the contribution to scattering from the upper bound co-spectrum (model 1) for wave numbers below k^* is thus given by $\sigma_v^{ST<}=\sigma_v^{T<}/R_{\rho c}+R_{\rho c}\sigma_v^{S<}=\sigma_v^T(2/R_{\rho c})$. The contribution to scattering from our co-spectrum [model 2: Eq. (39)] is $\sigma_v^{ST<}=\sigma_v^{T<}(1+L_e^{-1})(2/R_{\rho c})$ for wave numbers below k^*. Since $L_e \gg 1$, the contribution to scattering from σ_v^{ST} is approximately equal for both models and is determined by $2/|R_{\rho c}|$.

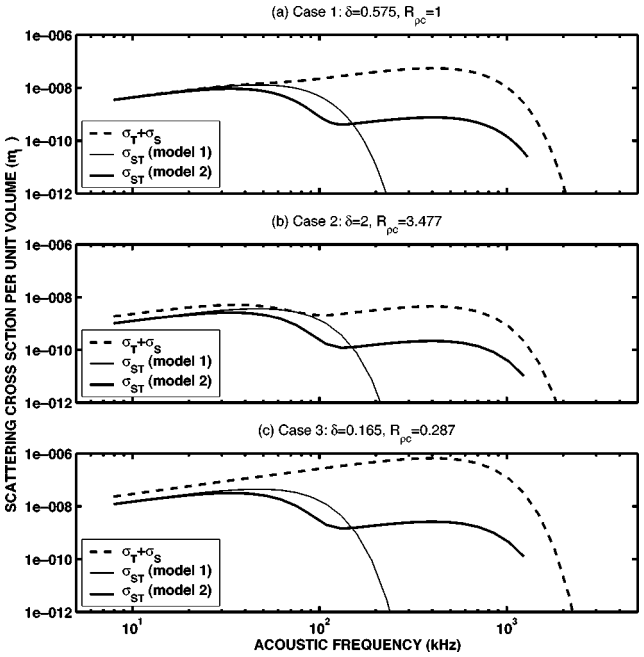

FIG. 4. The sum of the temperature and salinity contributions to the scattering cross section per unit volume $\sigma_v^T+\sigma_v^S$ (dashed line), the contribution to the scattering cross section per unit volume from the upper bound model for the co-spectrum σ_v^{ST} (model 1: thin line), and the contribution to the scattering cross section per unit volume from the co-spectrum model based on Stern's theory σ_v^{ST} (model 2: thick line). Predictions are plotted as a function of acoustic frequency, at backscattering, for model input parameters taken from Table I.

For wave numbers above k_d, $\sigma_v^S \gg \sigma_v^T$. Consequently, for the upper bound co-spectrum [model 1: Eq. (37)] $\sigma_v^{ST} = \sigma_v^S(R_{\rho c}/R_G)$, while for our co-spectrum [model 2: Eq. (39)] $\sigma_v^{ST} \approx \sigma_v^S(2R_{\rho c}/L_e)$. However, since R_G increases relatively rapidly, and $2R_{\rho c}/L_e \ll 1$ for typical values of $R_{\rho c}$ investigated here, the contribution to scattering from either co-spectrum, for wave numbers above k_d, is small. For the small range of wave numbers between approximately k^* and k_d, the wave number dependence of σ_v^{ST} is quite complicated, depending on a delicate balance set by the values of $R_{\rho c}$, R_G, L_e, and the relative magnitudes of σ_v^T and σ_v^S (Fig. 4).

Briefly synthesizing, the contribution from the co-spectrum does not, in general, significantly alter the scattering trends, particularly at wave numbers above k_d. The most significant changes are expected to occur over a small wave number range between k^* and k_d.

D. The angular dependence of scattering from temperature and salinity microstructure

The angular dependence of σ_v^T and σ_v^S (Fig. 5) is determined by both $R_{\rho c}$ and the acoustic wave number, k. However, the angular dependence is significantly more sensitive to changes in k than to changes in $R_{\rho c}$, since $R_{\rho c}$ only changes by a factor of 2 between forward and backscattering. For a fixed acoustic wave number, k, as θ changes from backscattering ($\theta=\pi$) to forward ($\theta=0$) scattering, the wave number K spans through the values from $K=2k$ to 0. There are three wave number regions that must be considered in order to understand the general angular trends in σ_v^S

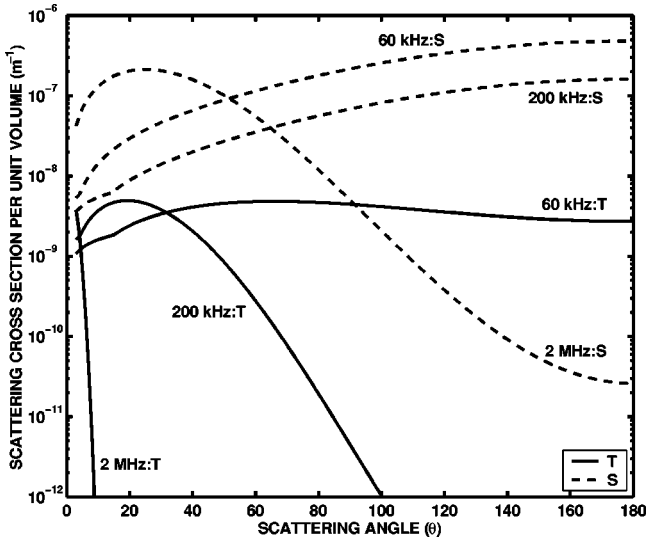

FIG. 5. The angular dependence of the temperature, σ_v^T, and salinity, σ_v^S, contributions to the scattering cross section per unit volume at (i) 60 kHz (region I: $k_d=769$ cpm, $k=251$ cpm, $K=502$ cpm at $\theta=\pi$), (ii) 200 kHz (region II: $k_d=769$ cpm, $k_{ds}=9207$ cpm, $k=838$ cpm, $K=1676$ cpm at $\theta=\pi$), and (iii) 2.3 MHz (region III: $k_{ds}=9207$ cpm, $k=9634$, $K=19268$ cpm at $\theta=\pi$), for model input parameters taken from case 3 in Table I.

and σ_v^T (Fig. 5): (i) $2k \leqslant k_d$, (ii) $k_d \leqslant 2k \leqslant k_{ds}$, and ($iii$) $2k \geqslant k_{ds}$. In region (i), the angular dependence of both σ_v^T and σ_v^S is relatively flat since $K=2k$ lies below the sharp roll-off in σ_v^T. In region (ii), σ_v^T depends very strongly on the scattering angle, while σ_v^S does not. At backscattering, $K=2k$ corresponds to wave numbers above the sharp roll-off in σ_v^T, and as the angle decreases towards forward scattering, the wave number K spans through the sharp roll-off, resulting in a strong angular dependence. In contrast, σ_v^S remains relatively flat since $K<k_{ds}$ for all angles. In region (iii), both σ_v^T and σ_v^S depend strongly on the multi-static scattering angle since $2k>k_{ds}>k_d$ and as θ changes from π to 0, K sweeps through the sharp roll-off in both the temperature and salinity. It is clear that the differences between the angular trends in σ_v^T and σ_v^S are largest in region (ii), where the wave number K at backscattering lies between the diffusive cutoff wave number for temperature and salinity. In fact, the vast differences predicted between the angular dependence of σ_v^S and σ_v^T in this region of wave number space suggest that multi-static measurements of acoustic scattering may provide a very fruitful technique for discriminating between temperature and salinity microstructure.

E. Acoustic scattering predictions based on high resolution microstructure data

In this section we make predictions of acoustic backscattering from oceanic microstructure based on data from which all the necessary model input parameters can be extracted. This data set involves microstructure data taken on the R/V NEW HORIZON in March 1991 on a cruise to the seamount Fieberling Guyot. A high resolution profiler (HRP) (Schmitt *et al.*, 1988) was deployed 95 times above and around the seamount, which rises from background depths of approximately 4000 m to about 500 m below the surface.

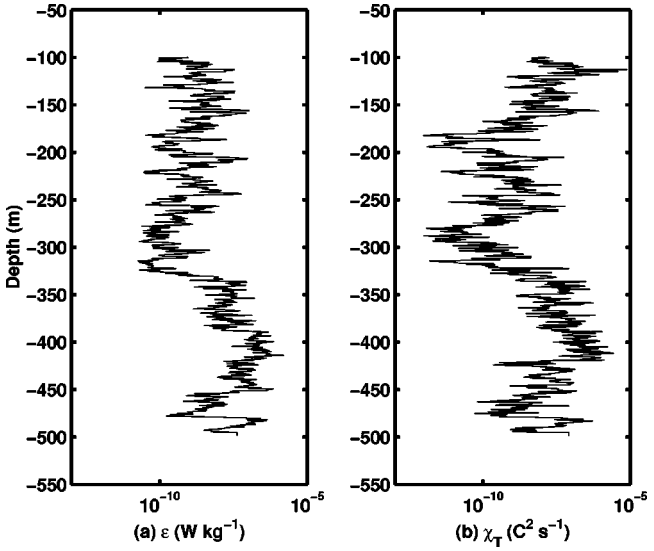

FIG. 6. Vertical profiles of (a) ϵ (W kg^{-1}) and (b) χ_T (°C^2 s^{-1}) performed with the HRP directly over the seamount summit Fieberling Guyot in 500 m of water. Dissipation rates just above the summit are significantly elevated. Profiles performed off the seamount shoulder (not shown here) show less structure and have uniformly lower values. The noise floor is typically around 10^{-11} (W kg^{-1}) for ϵ and 10^{-12} (°C^2 s^{-1}) for χ_T.

From the microstructure sensors on the HRP it is possible to obtain all the necessary model input parameters, at scales commensurate with the acoustic wavelengths of interest.

Acoustic scattering predictions were made for a large subset of the HRP profiles. We present results for a HRP profile performed directly above the seamount summit, since the microstructure measurements indicated that there were increased dissipation rates and velocity shear at the seamount summit, resulting in increased mixing and turbulence (Toole *et al.*, 1997) (Fig. 6). The acoustic scattering predictions reflect these observations, with elevated scattering levels predicted for both temperature and salinity microstructure over the seamount summit (Fig. 7). Over a broad frequency range, the predicted contribution to scattering from salinity microstructure just over the seamount summit is larger than the contribution from temperature microstructure. The results of our model also indicate that the contribution to scattering from the density term is at least as significant as the contribution from the sound speed term. There is a scattering layer between 350 and 450 m in which the predicted scattering levels from salinity microstructure (with approximately equal contributions from density and sound speed fluctuations) are similar in magnitude to typical scattering levels expected for zooplankton (Wiebe *et al.*, 1997). These results suggest that if the biological processes in the vicinity of the seamount could be accurately characterized, acoustic scattering techniques might provide a viable means to map areas of high turbulence.

V. SUMMARY AND CONCLUSIONS

In this paper we have extended the current theory of acoustic scattering from turbulent oceanic microstructure to include random fluctuations in density. Previously, it had been assumed that acoustic scattering from oceanic microstructure was due to sound speed fluctuations alone. We have predicted that the contribution to scattering from fluctuations in the density can be comparable to the contribution from sound speed fluctuations, under some circumstances. Depending on the scattering angle, the density contribution can increase the scattering levels by as much as 6 dB, resulting in peak scattering levels that, under certain conditions, could be comparable to levels typically observed for scattering from zooplankton. Neglecting to include the density term can consequently lead to a potentially significant underestimate of volume scattering strengths.

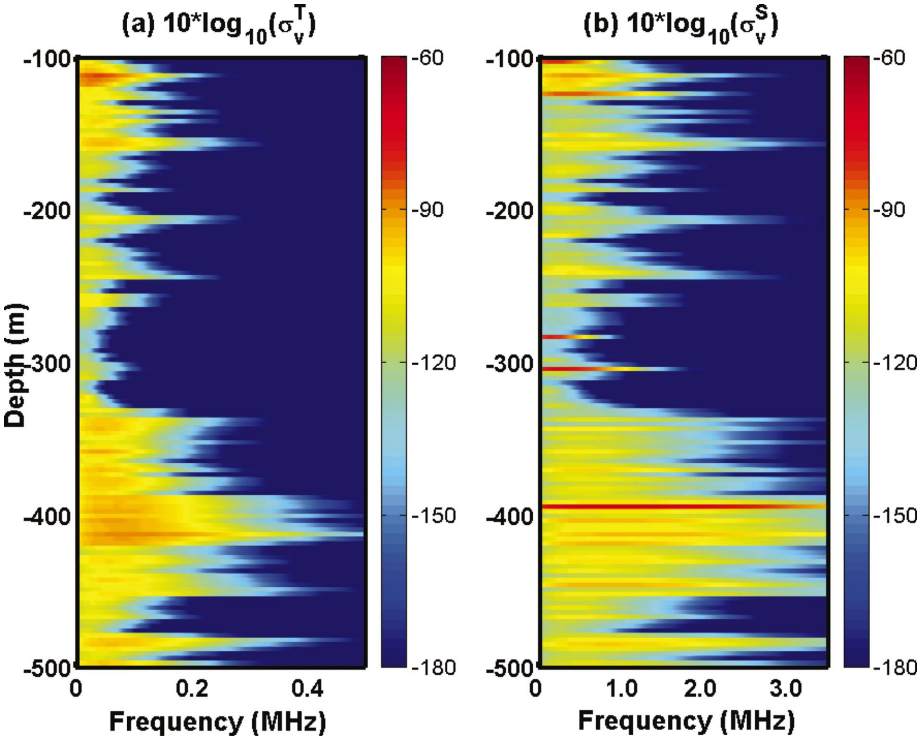

FIG. 7. Predicted contributions to backscattering from (a) temperature microstructure ($10\log_{10}\sigma_v^T$) and (b) salinity microstructure ($10\log_{10}\sigma_v^S$) as a function of depth and acoustic frequency based on HRP microstructure data obtained directly above the seamount Fieberling Guyot (see Fig. 6). The contribution to scattering from density fluctuations has been included in all scattering predictions. The contribution to scattering from the cospectrum (not shown) was found to be small. Note the different horizontal scales for temperature and salinity. There is a layer of elevated scattering just above the seamount summit, with levels that are comparable to those expected from typical zooplankton patches.

As with scattering from media variability in the atmosphere, the inclusion of the density term results in an expression for the scattering cross section per unit volume that is explicitly dependent on the multi-static scattering angle. We predict a very strong dependence on the multi-static scattering angle at certain acoustic wave numbers, and suggest that this dependence could be exploited to distinguish between the contribution to scattering from temperature and salinity microstructure.

The derivations presented here are based on far field weak scattering theory, for which the Born approximation is valid. One of the primary assumptions is that the medium variability is stationary and homogeneous, allowing a statistical description of the scattering in terms of the spatial Fourier transform of the correlation function of the medium variability, which is simply the 3D wave number spectrum of the medium variability. By relating the variability in the density and sound speed to fluctuations in temperature and salinity at the microstructure scale we have obtained an expression for the scattering cross section per unit volume in terms of the wave number spectra of temperature, salinity, and the co-spectrum of temperature and salinity. The assumption of isotropy also allows the 3D wave number spectra to be expressed in terms of the 1D wave number spectra, which are more representative of spectra derived from oceanographic measurements.

By assuming a 1D Batchelor spectrum for temperature and salinity, expressions for the scattering cross section per unit volume have been derived in terms of parameters such as the dissipation rates of turbulent kinetic energy, temperature and salt variance. We have found that the parameter $R_{\rho c}$ is critical in determining the relative contribution to scattering from temperature and salinity microstructure. $R_{\rho c}$ is defined in a manner similar to the density (R_ρ) and sound speed (R_c) ratios, but combines the effects of both vertical density and sound speed changes. $R_{\rho c}$ depends on the multi-static scattering angle, but not on the acoustic frequency. At angles close to forward scattering $R_{\rho c}$ is approximately equal to the vertical sound speed ratio R_c. However, at angles close to backscattering, $R_{\rho c}$ is approximately equal to $R_c/2$.

Two models for the co-spectrum of temperature and salinity have been used. The first expression represents an upper bound for the temperature and salinity co-spectrum. The second expression for the co-spectrum we have derived, and is based on the temperature-salinity covariance theory of Stern (1968). We have found that the contribution to scattering from either of the co-spectrum models tends to be smallest at spatial wave numbers above the diffusive cutoff wave number for heat. For wave numbers below this, the approximate contribution from the co-spectrum for either model is given by $2/R_{\rho c}$. If $R_{\rho c} \approx -1$, the contribution to scattering from the co-spectrum term can almost exactly cancel the contribution from the temperature and salinity terms combined, over a limited range of wave numbers. If $R_{\rho c} < 0$ (>0), the contribution to the scattering from the co-spectrum tends to reduce (increase) the magnitude of the scattering that results from the sum of the temperature and salinity contributions.

We have made scattering predictions based on generic model input parameter values that are typically for open ocean environments. In addition, scattering predictions based on high resolution microstructure measurements obtained in the vicinity of a seamount in the northeast subtropical Pacific ocean, Fieberling Guyot, have also been made. For these data, there are no free model input parameters outside of the initial model assumptions. Our results indicate that the layer of elevated turbulence above the seamount summit could give rise to significant scattering levels, comparable to those of typical zooplankton patches, particularly at higher wave numbers. The possibility that particulate scatterers, such as microbubbles, small zooplankton, or sand, may aggregate at the locations of energetic turbulence has not been considered in this analysis. Our predictions indicate that high-frequency acoustic scattering could be a viable technique, in combination with appropriate ground truthing, to map regions of elevated turbulent microstructure.

In conclusion, models such as the one presented here are important for the accurate interpretation of acoustic scattering data, though supporting physical and environmental information, gathered by any variety of techniques, will probably always be necessary for the unambiguous interpretation of high-frequency acoustic scattering data in terms of either physical or biological processes. However, before it is possible to fully capitalize on the acoustic scattering model presented here for scattering from turbulent oceanic microstructure, controlled field and laboratory testing and validation are necessary, in which the physical environment (temperature, conductivity, and fluid velocity) is characterized at least at the same resolution as the acoustic wave length, in addition to the adequate characterization of particulate scatterers that may be present in the areas of elevated turbulence.

ACKNOWLEDGMENTS

The authors would like to thank Harvey Seim (Marine Sciences Department, University of North Carolina Chapel Hill) for providing his code for calculating the backscattering cross section due to sound speed fluctuations. We would also like to thank Lou Goodman (Graduate School for Marine Science and Technology, University of Massachusetts Dartmouth) for invaluable discussions on the importance of density fluctuations in determining high-frequency acoustic scattering. This work was supported in part by ONR, NSF, and the Woods Hole Oceanographic Institution. This is Woods Hole Oceanographic Institution Contribution No. 10750.

Batchelor, G. K. (**1959**). ''Small-scale variation of convective quantities like temperature in a turbulent fluid,'' J. Fluid Mech. **5**, 113–133.

Bendat, J. S., and Piersol, A. G. (**1986**). *Random Data: Analysis and Measurements Procedures* (Wiley, New York).

Chernov, L. A. (**1960**). *Wave Propagation in a Random Medium* (McGraw-Hill, New York).

Chu, D., and Ye, Z. (**1999**). ''A phase-compensated distorted wave Born approximation representation of the bistatic scattering by weakly scattering objects: Application to zo-oplankton,'' J. Acoust. Soc. Am. **106**, 1732–1743.

Dillon, T. M., and Caldwell, D. R. (**1980**). ''The Batchelor spectrum and dissipation in the upper ocean,'' J. Geophys. Res. **85**, 1910–1916.

Farmer, D. M., and Smith, J. D. (**1979**). ''Tidal interaction of stratified flow with a sill in Knight inlet,'' Deep-Sea Res., Part A **27**, 239–254.

Farmer, D. M., and Armi, L. (**1999**). ''The generation and trapping of internal solitary waves over topography,'' Science **283**, 188–190.

Flatte, S. R., Dashen, R., Munk, W. H., Watson, K. M., and Zachariasen, F. (**1979**). *Sound Transmission through a Fluctuating Ocean* (Cambridge U. P., London), p. 5.
Goodman, L. (**1990**). ''Acoustic scattering from ocean microstructure,'' J. Geophys. Res. **95**, 11557–11573.
Goodman, L., and Kemp, K. A. (**1981**). ''Scattering from volume variability,'' J. Geophys. Res. **86**, 4083–4088.
Goodman, L., Oeschger, J., and Szargowicz, D. (**1992**). ''Ocean acoustics turbulence study: Acoustic scattering from a buoyant axisymmetric plume,'' J. Acoust. Soc. Am. **91**, 3212–3227.
Gregg, M. (**1984**). ''Entropy generation in the ocean by small-scale mixing,'' J. Phys. Oceanogr. **14**, 688–711.
Haury, L. R., Briscoe, M. G., and Orr, M. H. (**1979**). ''Tidally generated internal wave packets in Massachusetts Bay,'' Science **278**, 312–317.
Holliday, D. V., and Pieper, R. E. (**1995**). ''Bioacoustical oceanography at high frequencies,'' ICES J. Mar. Sci. **52**, 279–296.
Ishimaru, A. (**1978**). *Wave Propagation and Scattering in Random Media* (Academic, New York), Vol. 2.
Kraichnan, R. H. (**1953**). ''The scattering of sound in a turbulent medium,'' J. Acoust. Soc. Am. **25**, 1096–1104.
Lavery, A. C., Stanton, T. K., Chu, D., and McGehee, D. (**2002**). ''Three-dimensional modeling of acoustic backscattering from fluid-like zooplankton,'' J. Acoust. Soc. Am. **111**, 1197–1210.
Lhermitte, R., and Lemmin, U. (**1993**). ''Turbulent flow microstructures observed by sonar,'' Geophys. Res. Lett. **20**, 823–826.
McGehee, D. M., O'Driscoll, R. L., and Martin Traykovski, L. V. (**1998**). ''Effect of orientation on acoustic scattering from Antarctic krill at 120 kHz,'' Deep-Sea Res., Part II **45**, 1273–1294.
Medwin, H., and Clay, C. S. (**1998**). *Fundamentals of Acoustical Oceanography* (Academic, New York).
Menemenlis, D., and Farmer, D. M. (**1995**). ''Path-averaged measurements of turbulence beneath ice in the Arctic,'' J. Geophys. Res. **100**, 13655–13663.
Morse, P. M., and Ingard, K. U. (**1968**). *Theoretical Acoustics* (Princeton U. P., Princeton, NJ).
Munk, W. H., and Garrett, C. J. R. (**1973**). ''Internal wave breaking and microstructure,'' Boundary-Layer Meteorol. **4**, 37–45.
Oakey, N. S. (**1982**). ''Determination of the rate of dissipation of turbulent energy from simultaneous temperature and shear microstructure measurements,'' J. Phys. Oceanogr. **12**, 256–271.
Oeschger, J., and Goodman, L. (**1995**). ''Acoustic scattering from a thermally driven buoyant plume,'' J. Acoust. Soc. Am. **100**, 1421–1462.
Osborn, T., and Cox, C. S. (**1972**). ''Oceanic fine structure,'' Geophys. Fluid Dyn. **3**, 321–345.
Orr, M. H., Haury, L. R., Wiebe, P. H., and Briscoe, M. G. (**2000**). ''Backscatter of high-frequency (200 kHz) acoustic wave fields from ocean turbulence,'' J. Acoust. Soc. Am. **108**, 1595–1601.
Proni, J. R., and Apel, J. R. (**1975**). ''On the use of high-frequency acoustics for the study of internal waves and microstructure,'' J. Geophys. Res. **80**, 1147–1151.
Sandstrom, H., Elliott, J. A., and Cochrane, N. A. (**1989**). ''Observing groups of solitary internal waves and turbulence with BATFISH and Echo-Sounder,'' J. Phys. Oceanogr. **19**, 987–997.
Schmitt, R. W., Toole, J. M., Koehler, R. L., Mellinger, E. C., and Doherty, K. W. (**1988**). ''The development of a fine- and microstructure profiler,'' J. Atmos. Ocean. Technol. **5**, 484–500.
Seim, H. E. (**1999**). ''Acoustic backscatter from salinity microstructure,'' J. Atmos. Ocean. Technol. **16**, 1491–1498.
Seim, H. E., Gregg, M. C., and Miyamoto, R. T. (**1995**). ''Acoustic backscatter from turbulent microstructure,'' J. Atmos. Ocean. Technol. **12**, 367–380.
Stanton, T. K., Chu, D., and Wiebe, P. H. (**1998**). ''Sound scattering by several zooplankton groups. II. Scattering models,'' J. Acoust. Soc. Am. **103**, 236–253.
Stanton, T. K., Wiebe, P. H., Chu, D., and Goodman, L. (**1994**). ''Acoustic characterization and discrimination of marine zooplankton and turbulence,'' ICES J. Mar. Sci. **51**, 469–479.
Stern, M. E. (**1968**). ''T-S gradients on the micro-scale,'' Deep-Sea Res. Oceanogr. Abstr. **15**, 245–250.
Tatarski, V. I. (**1961**). *Wave Propagation in a Turbulent Medium* (McGraw-Hill, New York).
Thorpe, S. A., and Brubaker, J. M. (**1983**). ''Observation of sound reflection by temperature microstructure,'' Limnol. Oceanogr. **28**, 601–613.
Toole, J. M., Schmitt, R. W., Polzin, K. L., and Kunze, E. (**1997**). ''Near-boundary mixing above the flanks of a midlatitude seamount,'' J. Geophys. Res. **102**, 947–959.
Trevorrow, M. V. (**1998**). ''Observation of internal solitary waves near the Oregon coast using an inverted echo-sounder,'' J. Geophys. Res. **103**, 7671–7680.
Urick, R. J. (**1980**). *Principles of Underwater Sound*, 3rd ed. (McGraw-Hill, New York).
Waag, R. C. (**1984**). ''A review of tissue characterization from ultrasonic scattering,'' IEEE Trans. Biomed. Eng. **88**, 2418–2436.
Waag, R. C., Astheimer, J. P., and Swarthout, G. W. (**1985**). ''A characterization of wave-front distortion for analysis of ultrasound diffraction measurements made through an inhomogeneous medium,'' IEEE Trans. Sonics Ultrason. **32**, 36–48.
Waag, R. C., Dalecki, D., and Christopher, P. E. (**1989**). ''Spectral power determinations of compressibility and density variations in model media and calf liver using ultrasound,'' J. Acoust. Soc. Am. **85**, 423–431.
Washburn, L., Duda, T. F., and Jacobs, D. C. (**1996**). ''Interpreting conductivity microstructure: Estimating the temperature variance dissipation rate,'' J. Atmos. Ocean. Technol. **13**, 1166–1188.
Wiebe, P. H., Stanton, T. K., Benfield, M. C., Mountain, D. G., and Greene, C. H. (**1997**). ''High-frequency acoustic volume backscattering in the Georges Bank coastal region and its interpretation using scattering models,'' IEEE J. Ocean. Eng. **22**(3), 445–464.